Sinusoidal-Ripple-Current Charging Strategy and Optimal Charging Frequency Study for Li-Ion Batteries

Liang-Rui Chen, *Member, IEEE*, Shing-Lih Wu, *Student Member, IEEE*, Deng-Tswen Shieh, and Tsair-Rong Chen

***Abstract*—In this paper, the sinusoidal-ripple-current (SRC) charging strategy for a Li-ion battery is proposed. The ac-impedance analysis is used to explore the optimal charging frequency. Experiments indicate that the optimal charging performance can be achieved by the proposed SRC with the minimum-ac-impedance frequency $f_{Z\min}$. Compared with the conventional constant-current constant-voltage charging strategy, the charging time, the charging efficiency, the maximum rising temperature, and the lifetime of the Li-ion battery are improved by about 17%, 1.9%, 45.8%, and 16.1%, respectively.**

***Index Terms*—Li-ion battery, minimum ac impedance, sinusoidal ripple current (SRC).**

I. Introduction

THE development of portable electronic apparatus, electric vehicles, and renewable energies has been proliferating rapidly in recent years. A secondary battery is the significant and necessary energy-storage unit for these devices, and consequently, a high-quality battery charge strategy is desired. Nowadays, several charging techniques are proposed, such as constant-trickle-current charging, constant-current (CC) charging, and CC constant-voltage (CC-CV) charging [1]–[5]. Among them, the CC-CV is used most extensively, although its charging performance is still unable to meet the consumers' requirements of faster charging speed and longer lifetime. Thus, other charging techniques, such as fuzzy control, neural network, heredity algorithm, ant-group algorithm, and gray prediction, are applied to obtain a better battery-charging performance [6]–[11]. The circuit design based on the charging systems mentioned earlier is both complicated and expensive. Hence, the phase-locked-loop charging techniques were adopted to reach the goal of high performance and low cost [12]–[15].

Advanced battery-charging systems mostly use the technique of pulse charging which allows the evener distribution of ions in the battery electrolyte [16]–[25]. It meets the purpose of slowing down the polarization of the battery and advances the charge speed and the lifetime. Traditionally, the empirical method and the trial-and-error method are mostly used to search for the optimal charging frequency in the type of pulse charging system. The scientific method is not particularly used to explore how the optimal charging frequency of the Li-ion battery can be decided. In other words, to explore the optimal charging frequency of the Li-ion battery and to efficiently improve its charging performances are the most important tasks. Moreover, a low-frequency sinusoidal current effect in a one-stage charger with power factor correction was discussed [26]. Experiments show that the charging speed and the rising temperature of a lead–acid battery charged by a 100-Hz sinusoidal current seem little better than those charged by CC-CV [26]. In addition, the sinusoidal current charging for a $LiFePO_4$ battery was tested and obtained better charging performances [27]. For these reasons, the ac-impedance analysis is used in this paper to explore the optimal charging frequency. In addition, the sinusoidal-ripple-current (SRC) charging strategy for a Li-ion battery is also proposed. When the Li-ion battery is charged by the proposed SRC charging strategy with the minimum-ac-impedance frequency $f_{Z\min}$, an optimal charging performance can be obtained. Specially, the charging efficiency, the rising temperature, and the lifetime are obviously improved by using the proposed SRC with $f_{Z\min}$.

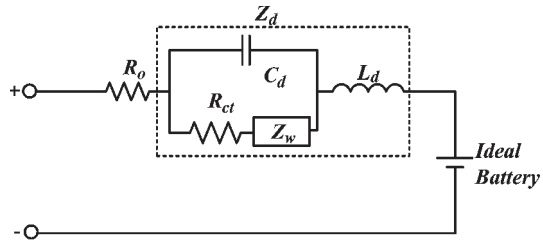

Fig. 1. Li-ion-battery ac-impedance model.

II. AC-Impedance Analysis

In the past few decades, ac-impedance analysis has been widely used in the research of electrochemistry. The ac impedance of a battery can be used to explore battery performance including state of charge and state of health [25]–[32]. Fig. 1 shows the Li-ion-battery ac-impedance model. This model consists of a charge transfer resistance $R_{\rm ct}$, a Warburg impedance

Manuscript received June 28, 2011; revised October 12, 2011 and December 10, 2011; accepted December 20, 2011. Date of publication January 26, 2012; date of current version September 6, 2012.

L.-R. Chen, S.-L. Wu, and T.-R. Chen are with the Department of Electrical Engineering, National Changhua University of Education, Changhua 500, Taiwan (e-mail: lrchen@cc.ncue.edu.tw; D95621005@cc.ncue.edu.tw).

D.-T. Shieh is with the Material and Chemical Research Laboratories, Industrial Technology Research Institute, Hsinchu 31040, Taiwan (e-mail: dts@itri.org.tw).

Color versions of one or more of the figures in this paper are available online at http://ieeexplore.ieee.org.

Digital Object Identifier 10.1109/TIE.2012.2186106

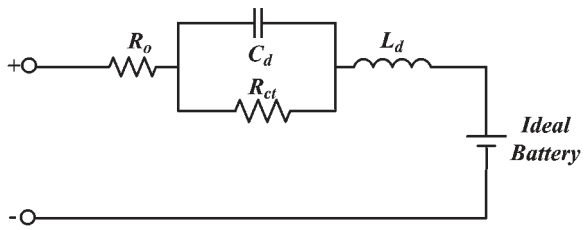

Fig. 2. Simplified Li-ion-battery impedance model.

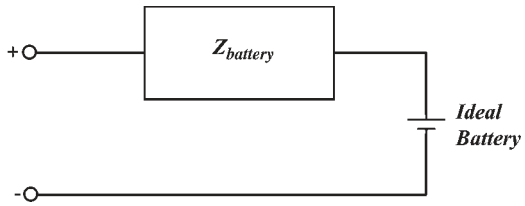

Fig. 3. Li-ion-battery equivalent circuit model.

Z_w, a double-layer capacitance C_d, an ohmic resistance R_o, and an anode inductance L_d [33]–[37]. The Warburg impedance Z_w influences the ac impedance only when the charging frequency is below 1 Hz. Therefore, the Warburg impedance Z_w can be neglected [38]. Fig. 2 shows the simplified Li-ion-battery ac-impedance model adopted in this paper. Fig. 3 shows the Li-ion battery's equivalent circuit model which consists of an ac impedance and an ideal battery. From the electrical circuit view, it is possible to find a frequency to minimize the battery impedance so as to reduce the energy loss in the battery-charging process. That means that the energy loss in electrical energy transfer to chemical energy is minimized. Therefore, a maximum energy transfer efficiency (i.e., the best electrochemical reaction) is obtained in the battery. In fact, it has been shown that a smaller charge transfer resistance means a better electrochemical reaction [39], [40], proving further that a better charge strategy can result in a smaller ohmic resistance [41].

Assuming that the charging frequency is f_s, the ac impedance of the battery Z_{battery} can be written as

$$Z_{\text{battery}}(\omega_s) = \left[R_o + \frac{\frac{R_{\text{ct}}}{(\omega_s C_d)^2}}{R_{\text{ct}}^2 + \left(\frac{1}{\omega_s C_d}\right)^2} \right] + j \left[\omega_s L_d - \frac{\frac{R_{\text{ct}}^2}{\omega_s C_d}}{R_{\text{ct}}^2 + \left(\frac{1}{\omega_s C_d}\right)^2} \right] \quad (1)$$

according to Fig. 2. Note that the temperature impact in this mathematic analysis is ignored. Clearly, the ac impedance of a Li-ion battery is changed as a consequence of the charging frequency. The frequency $f_{Z\min}$ that corresponds to the minimum ac impedance $Z_{\min}$ can also be obtained and shown as

$$f_{Z\min} = \frac{1}{2\pi R_{\text{ct}} C_d} \sqrt{K-1} \quad (2)$$

where

$$K = \frac{\sqrt{2R_o R_{\text{ct}}^3 C_d^2 + 2L_d R_{\text{ct}}^2 C_d + R_{\text{ct}}^4 C_d^2}}{L_d}. \quad (3)$$

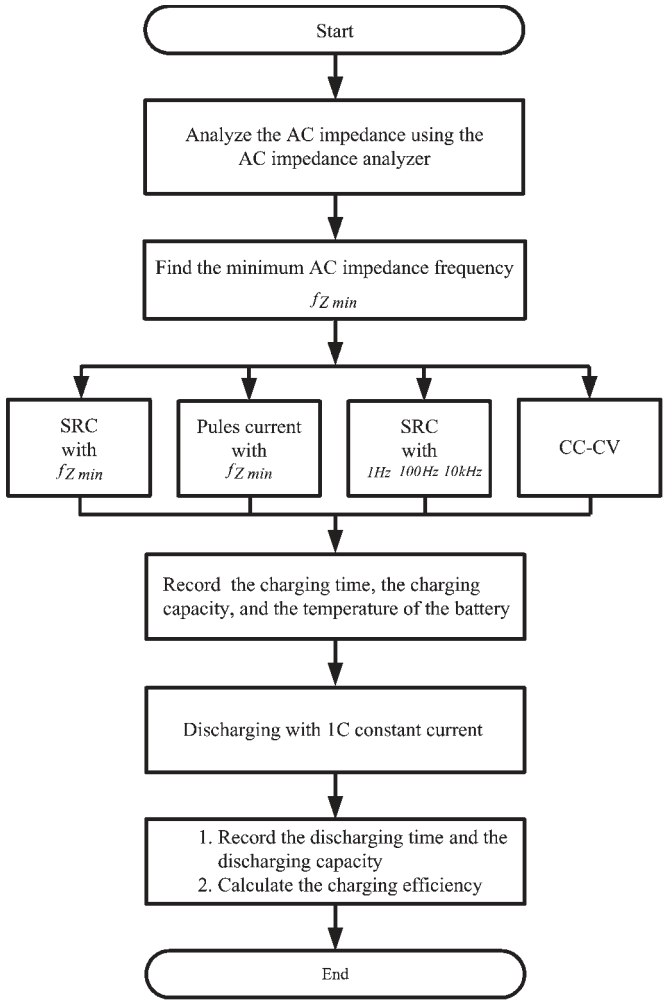

Fig. 4. Flowchart of the experiment.

The minimum ac impedance $Z_{\min}$ can also be obtained and shown as

$$Z_{\min}^2 = R_o^2 + \left(\frac{L_d}{R_{\text{ct}} C_d}\right)^2 (\sqrt{K}-1) + \frac{2R_o R_{\text{ct}} + R_{\text{ct}}^2}{\sqrt{K}} - 2\frac{L_d}{C_d}\left(1 - \frac{1}{\sqrt{K}}\right). \quad (4)$$

III. Experimental Process and Test Platform

Fig. 4 shows the flowchart of the battery-charging test in this paper. First, the ac-impedance spectrum of the Li-ion battery is obtained with an ac-impedance analyzer. According to the ac-impedance spectrum, the minimum-ac-impedance frequency $f_{Z\min}$ can be obtained. Then, the Li-ion battery is charged by the proposed SRC with $f_{Z\min}$. When the battery is charged, the charging time, the charging capacity, and the temperature are recorded simultaneously. When the open-circuit voltage of the Li-ion battery reaches 4.2 V, the Li-ion battery is regarded as fully charged and then rests for 1 h. After that, the Li-ion battery is discharged with 1-C CC by using an electronic load until the battery voltage reaches 3 V. Meanwhile, the discharging

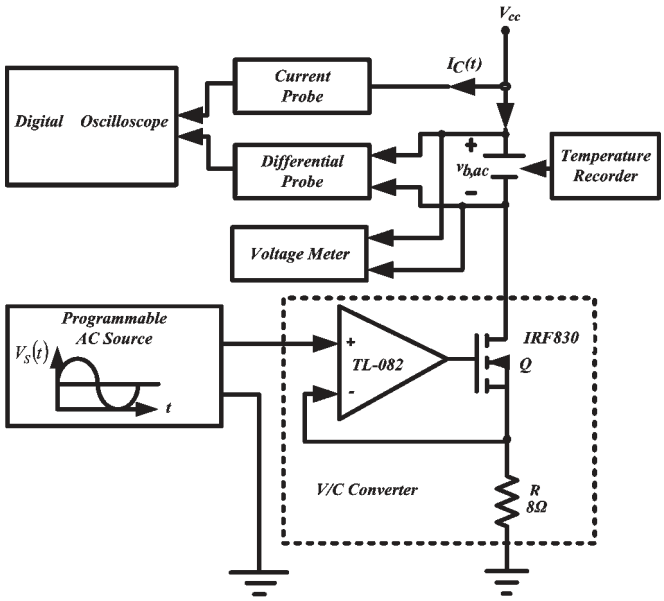

Fig. 5. Battery-charging test platform.

time and discharging capacity are recorded. Finally, the battery-charging efficiency is calculated according to

$$\eta(\%) = \frac{Q_{\text{out}}}{Q_{\text{in}}} \times 100\% \tag{5}$$

where Q_{in} is the charging capacity and Q_{out} is the discharging capacity.

In order to verify that the battery-charging performance is improved under the optimal charging frequency, the SRC with four charging frequencies, which are 1 Hz, 100 Hz, $f_{Z\,\min}$, and 10 kHz, is also tested. In addition, pulse current and CC-CV are also included. Fig. 5 shows the battery-charging test platform that consists of a digital oscilloscope, a programmable ac source, and a voltage/current converter which contains a MOSFET and an operational amplifier. First, a programmable ac source is used to produce sinusoidal ripple signals $V_S(t)$ shown as follows:

$$V_S(t) = V_{\text{avg}} + V_{\text{avg}} \sin 2\pi f_s t \tag{6}$$

in which V_{avg} is the average voltage of $V_S(t)$. The SRC for charging the Li-ion battery can be generated by the voltage/current converter and shown as

$$I_C(t) = \frac{V_S(t)}{R} = \frac{V_{\text{avg}} + V_{\text{avg}} \sin 2\pi f_s t}{R} \tag{7}$$

where R is a current-set resistor. When the battery is charging, the digital oscilloscope is used to get the wave of the charging current and the charging voltage. Meanwhile, the charging time, the charging capacity, and the rising temperature are also measured and recorded. Fig. 6(a) and (b) shows the actual pictures of the battery-charging test platform and the ac-impedance analyzer. The used apparatus are listed in Table I.

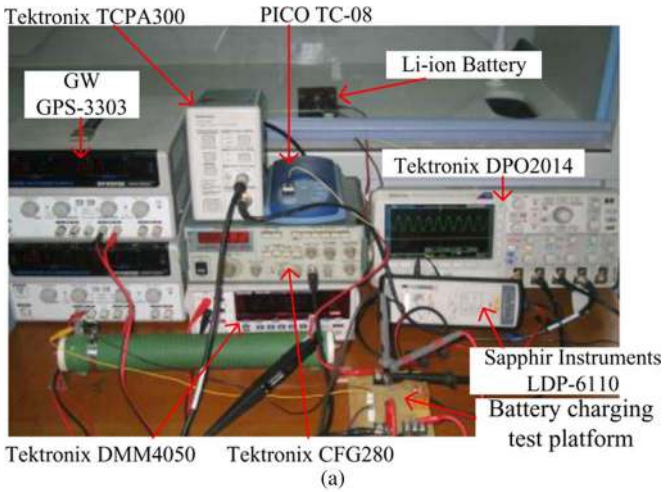

Fig. 6. Pictures of (a) the battery-charging test platform and (b) the ac-impedance analyzer.

TABLE I
APPARATUS

Apparatus	Type
Current Probe	Tektronix TCPA300
Differential Probe	Sapphir Instruments LDP-6110
Digital Oscilloscope	Tektronix DPO 2014
Programmable AC Source	Tektronix CFG280
Temperature Recorder	Pico TC-08
Power Supply	GW instek GPS-3303
Voltage Meter	Tektronix DMM4050
AC Impedance Analyzer	Solartron 1280B

IV. EXPERIMENTAL RESULTS

Three brand-new SANYO UR18650W 1500-mAh high-power Li-ion batteries, named batteries A, B, and C, are used to verify the proposed SRC performance in this paper. Fig. 7 shows the ac-impedance spectrum of battery A measured by

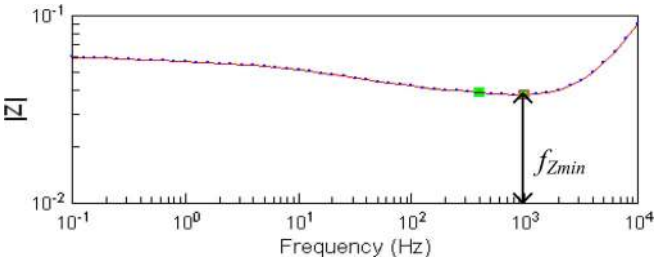

Fig. 7. Measured ac-impedance spectrum of battery A.

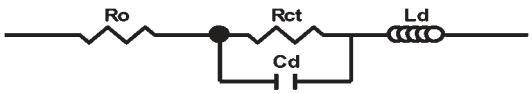

Element	Freedom	Value
Ro	Free(+)	0.03615
Rct	Free(+)	0.02251
Cd	Free(+)	0.03567
Ld	Free(+)	1.4516E-6

Fig. 8. Indirectly estimated parameters of battery A.

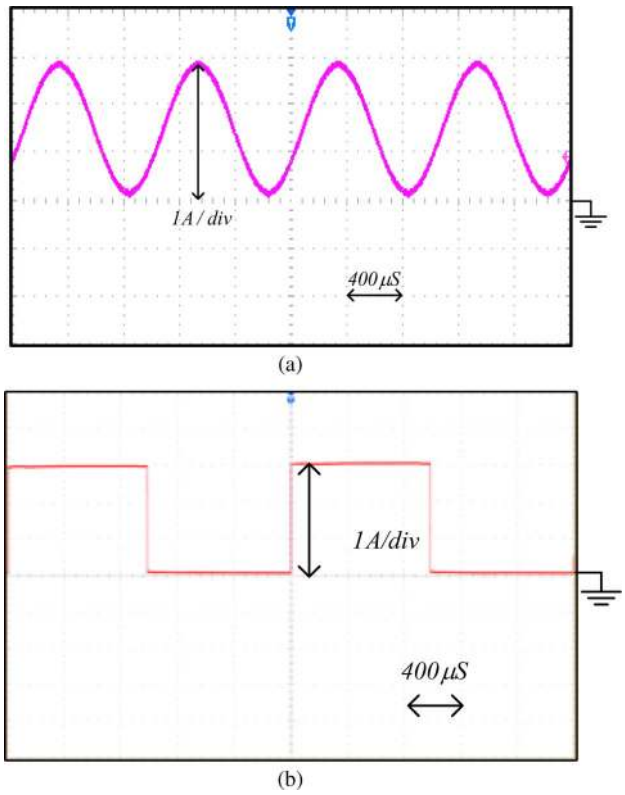

Fig. 9. (a) SRC charging current. (b) Pulse charging current.

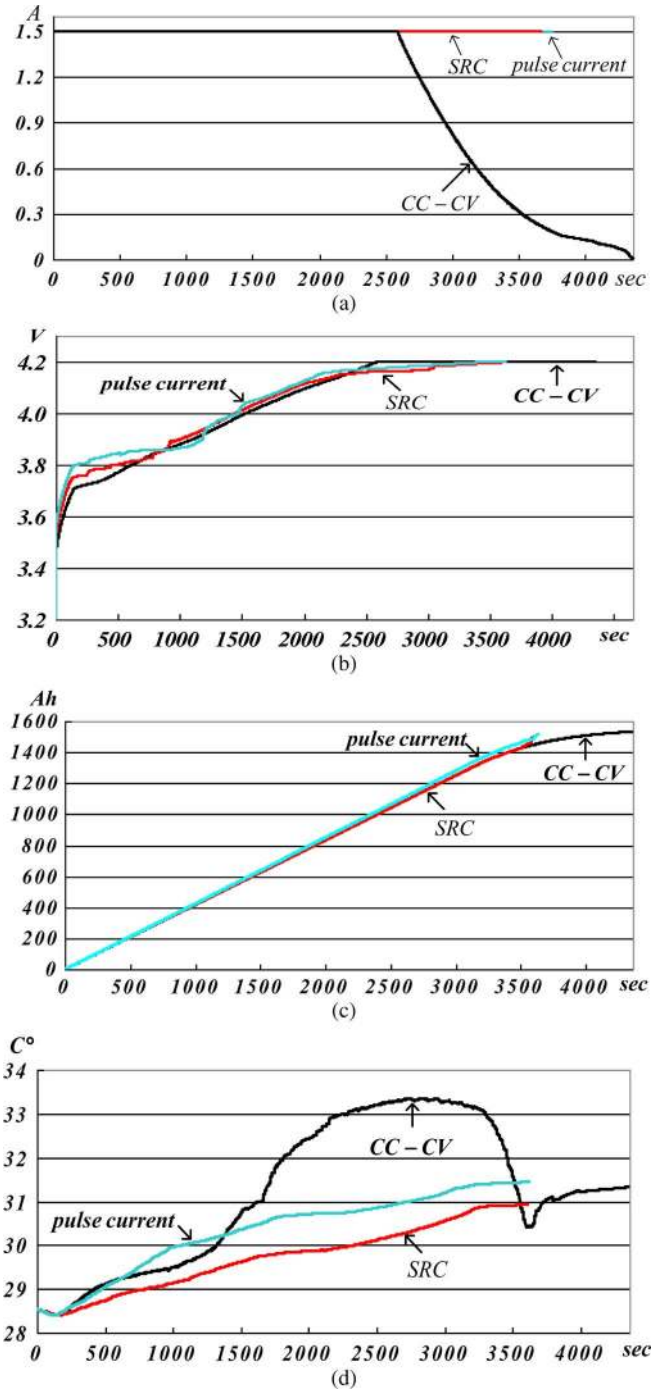

Fig. 10. (a) Charging current curves. (b) Charging voltage curves. (c) Charging capacity curves. (d) Temperature curves.

the ac-impedance analyzer Solartron 1280B. The ac-impedance spectrum indicates that the minimum-ac-impedance frequency $f_{Z\min}$ and the minimum ac impedance $Z_{\min}$ are about 998 Hz and 0.0384 Ω, respectively.

These values of the transfer resistance $R_{\rm ct}$, the double-layer capacitance C_d, the ohmic resistance R_o, and the anode inductance L_d can be indirectly estimated by the ac-impedance analyzer Solartron 1280B and are shown in Fig. 8. Using (2) and (4), the minimum-ac-impedance frequency $f_{Z\min}$ and the minimum ac impedance $Z_{\min}$ are calculated and obtained as 992 Hz and 0.0382 Ω, respectively. Clearly, the theoretical results are very close to the experimental results. This indicates that the mathematical analysis and the practical measurement are in agreement.

Fig. 9(a) shows the generated SRC charging current of the used battery-charging test platform. Clearly, the proposed SRC waveform can be excellently generated, and the average charging current of the SRC is 1.5 A (i.e., 1 C). Fig. 9(b) shows the generated pulse charging current of the used battery-charging test platform. The average of the pulse charging current is also 1.5 A (i.e., 1 C).

TABLE II
EXPERIMENTAL RESULTS OF BATTERY A CHARGED BY THE SRC WITH DIFFERENT FREQUENCIES

Charge Method	SRC			
frequency (Hz)	1	100	f_{Zmin} 998	10k
Charging Time (sec)	3645	3639	3627	3669
Charging Capacity (Ah)	1.52	1.52	1.51	1.53
Discharging Time (sec)	3588	3588	3589	3558
Discharging Capacity(Ah)	1.50	1.50	1.50	1.48
Efficiency (%)	98.4	98.6	99.0	97.0
Rising Temperature (°C)	3.3	3.2	2.4	3.6

TABLE III
EXPERIMENTAL RESULTS OF BATTERY A CHARGED BY THE PULSE CURRENT WITH DIFFERENT FREQUENCIES

Charge Method	Pulse current			
frequency (Hz)	1	100	f_{Zmin} 998	10k
Charging Time (sec)	3659	3646	3637	3681
Charging Capacity (Ah)	1.52	1.52	1.52	1.53
Discharging Time (sec)	3586	3586	3586	3558
Discharging Capacity (Ah)	1.49	1.49	1.49	1.49
Efficiency (%)	98	98.3	98.6	96.6
Rising Temperature (°C)	3.4	3.4	2.9	3.6

TABLE IV
EXPERIMENTAL RESULTS OF BATTERY A CHARGED BY CC-CV

Charge Method	CC-CV
Charging Time (sec)	4362
Charging Capacity (Ah)	1.5
Discharging Time (sec)	3497
Discharging Capacity (Ah)	1.457
Efficiency (%)	97
Rising Temperature (°C)	4.7

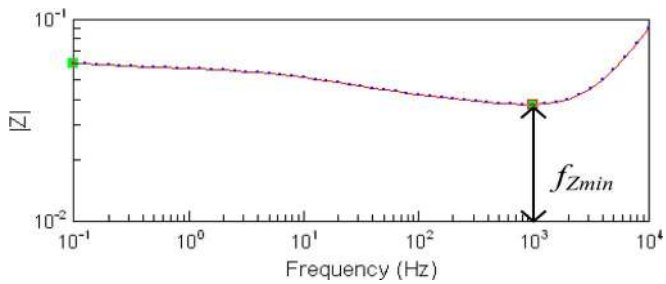

Fig. 11. Measured ac-impedance spectrum of battery B.

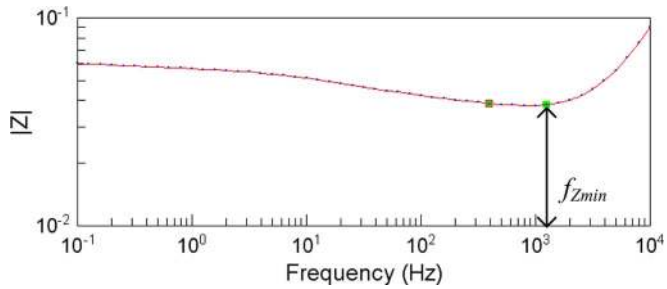

Fig. 12. Measured ac-impedance spectrum of battery C.

The charging current, voltage, capacity, and temperature curves of the proposed SRC with $f_{Z\min}$, the standard CC-CV, and the pulse-current charging with $f_{Z\min}$ in a fully charging cycle are shown in Fig. 10(a)–(d), respectively. Clearly, the proposed SRC has the best performance in charging speed, charging efficiency, and rising temperature in these three charging methods. More details of the experimental results are described as follows.

Table II shows the experimental results of battery A charged by the SRC with 1 Hz, 100 Hz, $f_{Z\min}$, and 10 kHz. We can find different charging frequency results in different charger performances. However, battery A charged with $f_{Z\min}$ has the fastest charging speed, the maximum charging efficiency, and the minimum rising temperature. Tables III and IV show the experimental results of battery A charged by the pulse current with $f_{Z\min}$ and by the CC-CV. In the pulse-current charging strategy, the duty cycle is 50%, and the average charging current is 1.5 A, which is the same as that used in SRC. In the CC-CV charging strategy, the CC is also 1.5 A, and the constant voltage is 4.2 V.

Tables III and IV indicate that the charging speed, charging efficiency, and rising temperature of the pulse charging are all better than those of CC-CV. However, the battery-charging performance of the pulse charging is worse than that of the proposed SRC. Comparing Tables II–IV, we can see that the charging speed, the charging efficiency, and the rising temperature of battery A charged by the SRC are better than those of battery A charged by the pulse current and CC-CV.

Figs. 11 and 12 show the ac-impedance spectra of batteries B and C. The ac-impedance spectra indicate that the minimum-ac-impedance frequencies $f_{Z\min}$ are about 996 and 1238 Hz for batteries B and C, respectively. The minimum ac impedances $Z_{\min}$ of batteries B and C are about 0.0385 and 0.0385 Ω, respectively. We find that the minimum-ac-impedance frequency $f_{Z\min}$ varies for different Li-ion batteries.

Tables V–X show the charging time, the charging capacity, the discharging time, the discharging capacity, the charging efficiency, and the rising temperature of batteries B and C charged by the proposed SRC, the pulse current, and the CC-CV. It is clear that the proposed SRC with $f_{Z\min}$ has the fastest

TABLE V
EXPERIMENTAL RESULTS OF BATTERY B CHARGED BY THE SRC WITH DIFFERENT FREQUENCIES

Charge Method	SRC			
frequency (Hz)	1	100	f_{Zmin} 996	10k
Charging Time (sec)	3654	3644	3632	3673
Charging Capacity (Ah)	1.52	1.52	1.51	1.53
Discharging Time (sec)	3584	3584	3585	3568
Discharging Capacity(Ah)	1.49	1.49	1.49	1.49
Efficiency (%)	98.1	98.4	98.7	97.2
Rising Temperature (°C)	3.2	3.2	2.3	3.5

TABLE VI
EXPERIMENTAL RESULTS OF BATTERY B CHARGED BY THE PULSE CURRENT WITH DIFFERENT FREQUENCIES

Charge Method	Pulse current			
frequency (Hz)	1	100	f_{Zmin} 996	10k
Charging Time (sec)	3662	3650	3637	3686
Charging Capacity (Ah)	1.52	1.52	1.51	1.53
Discharging Time (sec)	3585	3585	3584	3562
Discharging Capacity (Ah)	1.49	1.49	1.49	1.48
Efficiency (%)	97.9	98.3	98.5	96.7
Rising Temperature (°C)	3.3	3.2	2.7	3.6

TABLE VII
EXPERIMENTAL RESULTS OF BATTERY B CHARGED BY CC-CV

Charge Method	CC-CV
Charging Time (sec)	4365
Charging Capacity (Ah)	1.51
Discharging Time (sec)	3520
Discharging Capacity (Ah)	1.467
Efficiency (%)	97.1
Rising Temperature (°C)	4.1

TABLE VIII
EXPERIMENTAL RESULTS OF BATTERY C CHARGED BY THE SRC WITH DIFFERENT FREQUENCIES

Charge Method	SRC			
frequency (Hz)	1	100	f_{Zmin} 1238	10k
Charging Time (sec)	3643	3637	3620	3669
Charging Capacity (Ah)	1.52	1.52	1.51	1.53
Discharging Time (sec)	3585	3586	3589	3568
Discharging Capacity(Ah)	1.49	1.49	1.50	1.49
Efficiency (%)	98.4	98.6	99	97.2
Rising Temperature (°C)	3.1	2.9	2.4	3.4

TABLE IX
EXPERIMENTAL RESULTS OF BATTERY C CHARGED BY THE PULSE CURRENT WITH DIFFERENT FREQUENCIES

Charge Method	Pulse current			
frequency (Hz)	1	100	f_{Zmin} 1238	10k
Charging Time (sec)	3656	3643	3631	3683
Charging Capacity (Ah)	1.52	1.52	1.51	1.53
Discharging Time (sec)	3588	3589	3588	3565
Discharging Capacity (Ah)	1.49	1.49	1.50	1.48
Efficiency (%)	98.1	98.5	98.8	96.8
Rising Temperature (°C)	3.1	3	2.9	3.4

TABLE X
EXPERIMENTAL RESULTS OF BATTERY C CHARGED BY CC-CV

Charge Method	CC-CV
Charging Time (sec)	4378
Charging Capacity (Ah)	1.5
Discharging Time (sec)	3489
Discharging Capacity (Ah)	1.453
Efficiency (%)	96.8
Rising Temperature (°C)	4.3

charging speed, the optimal charging efficiency, and the minimum rising temperature.

Tables XI–XIII show the average value of the charging time and the average value of the charging efficiency of three SANYO UR18650W 1500-mAh high-power Li-ion batteries charged by 1 Hz, 100 Hz, $f_{Z\min}$, and 10 kHz, respectively.

Table XIV lists the average experimental values of these three Li-ion batteries charged by CC-CV, the pulse current with $f_{Z\min}$, and the proposed SRC with $f_{Z\min}$. It is clear that the proposed SRC with $f_{Z\min}$ is the best among these three charge strategies. The average charging time, the average efficiency, and the average rising temperature of the proposed

TABLE XI
AVERAGING EXPERIMENTAL VALUES OF THESE THREE LI-ION BATTERIES CHARGED BY THE SRC

Charge Method	SRC			
frequency (Hz)	1	100	f_{Zmin}	10k
Charging Time (sec)	3647	3640	3626	3670
Charging Capacity (Ah)	1.52	1.52	1.51	1.53
Discharging Time (sec)	3586	3586	3588	3565
Discharging Capacity(Ah)	1.49	1.49	1.50	1.49
Efficiency (%)	98.3	98.5	98.9	97.1
Rising Temperature (°C)	3.2	3.1	2.4	3.5

TABLE XII
AVERAGING EXPERIMENTAL VALUES OF THESE THREE LI-ION BATTERIES CHARGED BY THE PULSE CURRENT

Charge Method	Pulse current			
frequency (Hz)	1	100	f_{Zmin}	10k
Charging Time (sec)	3659	3646	3635	3683
Charging Capacity (Ah)	1.52	1.52	1.51	1.53
Discharging Time (sec)	3586	3587	3586	3562
Discharging Capacity (Ah)	1.49	1.49	1.49	1.48
Efficiency (%)	98.0	98.4	98.6	96.7
Rising Temperature (°C)	3.3	3.2	2.8	3.5

TABLE XIII
AVERAGING EXPERIMENTAL VALUES OF THESE THREE LI-ION BATTERIES CHARGED BY CC-CV

Charge Method	CC-CV
Charging Time (sec)	4368
Charging Capacity (Ah)	1.50
Discharging Time (sec)	3502
Discharging Capacity (Ah)	1.46
Efficiency (%)	97.0
Rising Temperature (°C)	4.4

SRC with $f_{Z\min}$ are 3626 s, 98.9%, and 2.4 °C. Compared with the conventional CC-CV, the charging time, the efficiency, and the rising temperature are improved by about 17%, 1.9%, and 45.8%, respectively. Compared with the pulse current, the charging time, the efficiency, and the rising temperature are improved by about 0.24%, 0.27%, and 16.47%, respectively. It is interesting that little enhancement of the charging efficiency can obtain obvious improvement of the rising temperature.

TABLE XIV
AVERAGING EXPERIMENTAL VALUES OF THESE THREE LI-ION BATTERIES CHARGED BY CC-CV, THE PULSE CURRENT WITH $f_{Z\min}$, AND THE PROPOSED SRC WITH $f_{Z\min}$

Charge Method	CC-CV	Pulse current with f_{Zmin}	SRC with f_{Zmin}
Charging Time (sec)	4368	3635	3626
Efficiency (%)	97	98.6	98.9
Rising Temperature (°C)	4.4	2.8	2.4

Finally, the battery lifetime is also verified, and the deterioration curves charged by the proposed SRC with $f_{Z\min}$ and the conventional CC-CV during 1000 cycles are shown in Fig. 13. It is easy to see that the Li-ion-battery capacities charged by SRC and CC-CV are deteriorated to 93.4% and 89.9% for 1000 cycles, respectively. The CC-CV's resultant capacity after 839 cycles is equal to that of SRC after 1000 cycles according to the picture. This means that the lifetime is improved by about 16.1% by the proposed SRC as we wanted.

In order to analyze the $f_{Z\min}$ distribution, 28 brand-new 1500-mAh high-power Li-ion batteries are tested with different states of charge and ambient temperatures, and its distributions are shown in Fig. 14(a)–(d). We can find that a fully charge battery and a fully discharge battery have higher ac impedance. However, the $f_{Z\min}$ is varied with very little. On the other hand, a higher ambient temperature has a lower ac impedance for each battery. Still, the $f_{Z\min}$ is varied with very little.

The minimum-ac-impedance frequencies $f_{Z\min}$ are within 900 to 1200 Hz. This means that a fixed frequency can be set in a practical SRC charger to obtain a near-optimal charging performance. However, developing an online adaptive tuning algorithm to find $f_{Z\min}$ is necessary and worth to study in the future. For electrical vehicles [19], [30], [42]–[44], renewable-energy applications [45], [46], and other industrial applications [44], [47], [48], the using cost (i.e., battery price or battery life) can be obviously reduced by using the proposed SRC. Additionally, lower battery rising temperature results in higher safety for these application systems.

In this paper, the proposed SRC is discussed for a single Li-ion battery. However, the $f_{Z\min}$ of a battery pack can also be obtained by using an ac-impedance analyzer, and the proposed SRC can also charge series-connected Li-ion batteries.

V. CONCLUSION

In this paper, the SRC charging strategy for a Li-ion battery has been proposed and tested successfully. The ac-impedance spectrum is used to explore the optimal charging frequency. Experiments indicate that an excellent charging performance can be obtained by the proposed SRC with the minimum-ac-impedance frequency $f_{Z\min}$. Compared with the conventional CC-CV charging strategy, the charging time, the charging ef-

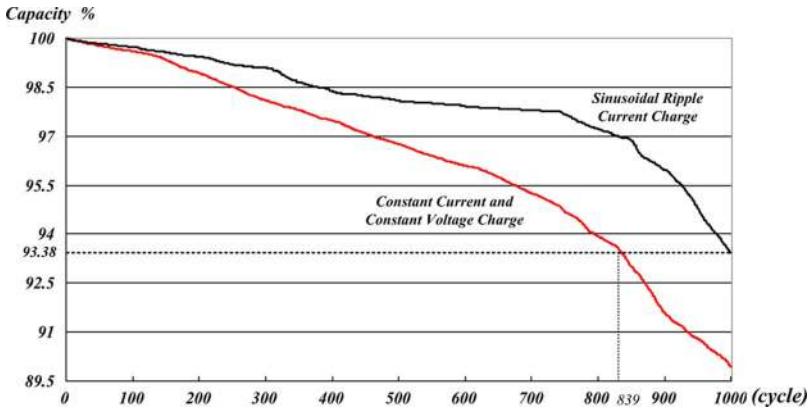

Fig. 13. Deterioration curves charged by SRC and CC-CV.

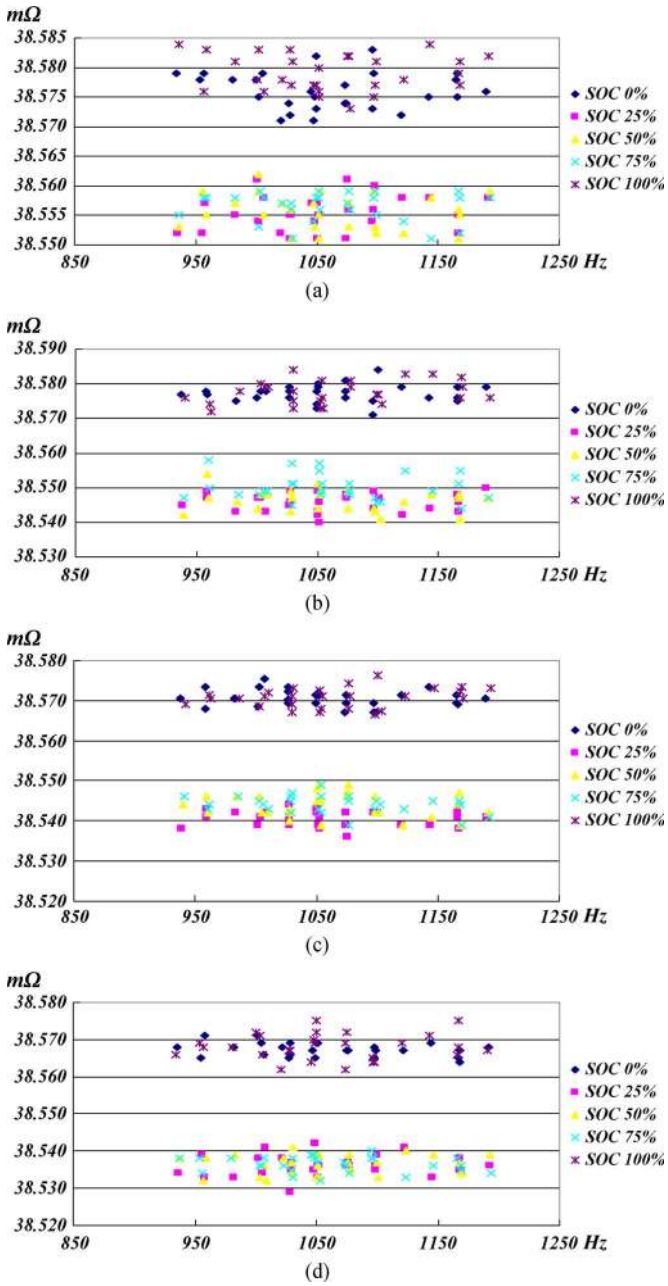

Fig. 14. $f_{Z\min}$ distributions for ambient temperatures of (a) 30 °C, (b) 40 °C, (c) 50 °C, and (d) 60 °C.

ficiency, the maximum rising temperature, and the lifetime of the Li-ion battery are improved by about 17%, 2%, 45.8%, and 16.1%, respectively. Compared with the traditional pulse-current charging strategy, the charging time, the charging efficiency, and the maximum rising temperature of the Li-ion battery are improved by about 0.24%, 0.27%, and 16.47%, respectively.

APPENDIX

The impedance Z_{battery} as shown in Fig. 2 can be written as

$$Z_{\text{battery}}(\omega_s) = \left[R_o + \frac{\frac{R_{\text{ct}}}{(\omega_s C_d)^2}}{R_{\text{ct}}^2 + \left(\frac{1}{\omega_s C_d}\right)^2}\right] + j\left[\omega_s L_d - \frac{\frac{R_{\text{ct}}^2}{\omega_s C_d}}{R_{\text{ct}}^2 + \left(\frac{1}{\omega_s C_d}\right)^2}\right] \tag{A-1}$$

and its square can be shown as

$$|Z_{\text{battery}}|^2 = A^2 + B^2 \tag{A-2}$$

where

$$A = \left[R_o + \frac{R_{\text{ct}}}{R_{\text{ct}}^2\omega_s^2 C_d^2 + 1}\right]^2 \tag{A-3}$$

$$B(\omega_s) = \left[\omega_s L_d - \frac{R_{\text{ct}}^2\omega_s C_d}{R_{\text{ct}}^2\omega_s^2 C_d^2 + 1}\right]^2. \tag{A-4}$$

Then, the differential equation of (A-2) can be obtained and written as

$$\frac{d|Z_{\text{battery}}|^2}{d\omega_s} = \frac{1}{2}\left(2A\left[\frac{-2R_{\text{ct}}E}{(D+1)^2}\right] + 2B\left[L_d - \frac{F(1-D)}{(D+1)^2}\right]\right) \tag{A-5}$$

where

$$D = R_{\text{ct}}^2\omega_s^2 C_d^2 \tag{A-6}$$

$$E = R_{\text{ct}}^2\omega_s C_d^2 \tag{A-7}$$

$$F = R_{\text{ct}}^2 C_d. \tag{A-8}$$

Next, make $d|Z_{\rm battery}|^2/d\omega_s = 0$ for obtaining the $|Z_{\rm battery}|^2$ minimum value, and the following equation can be obtained:

$$\frac{L_d^2}{R_{\rm ct}C_d}D^2 + \frac{3L_d^2}{R_{\rm ct}C_d}D^2 + \left(\frac{3L_d^2}{R_{\rm ct}C_d} - 2R_oF - 2L_dR_{\rm ct} - R_{\rm ct}F\right)D + \left(\frac{L_d^2}{R_{\rm ct}C_d} - 2R_oF - 2L_dR_{\rm ct} - F\right) = 0. \quad \text{(A-9)}$$

After that, the minimum-ac-impedance frequency can be obtained and shown as

$$f_{Z\,\min} = \frac{1}{2\pi R_{\rm ct}C_d}\sqrt{K-1} \quad \text{(A-10)}$$

where

$$K = \frac{\sqrt{2R_oR_{\rm ct}^3C_d^2 + 2L_dR_{\rm ct}^2C_d + R_{\rm ct}^4C_d^2}}{L_d}. \quad \text{(A-11)}$$

Finally, the minimum ac impedance $Z_{\min}$ can also be obtained as follows:

$$Z_{\min}^2 = R_o^2 + \left(\frac{L_d}{R_{\rm ct}C_d}\right)^2(\sqrt{K}-1) + \frac{2R_oR_{\rm ct} + R_{\rm ct}^2}{\sqrt{K}} - 2\frac{L_d}{C_d}\left(1 - \frac{1}{\sqrt{K}}\right). \quad \text{(A-12)}$$

REFERENCES

[1] R. C. Cope and Y. Podrazhansky, "The art of battery charging," in *Proc. 14th Battery Conf. Appl. Adv.*, Long Beach, CA, Jan. 1999, pp. 233–235.

[2] B. D. Valle, C. T. Wentz, and R. Sarpeshkar, "An area and power-efficient analog Li-ion battery charger circuit," *IEEE Trans. Biomed. Circuits Syst.*, vol. 5, no. 2, pp. 131–137, Apr. 2011.

[3] C. H. Lin, C. Y. Hsieh, and K. H. Chen, "A Li-ion battery charger with smooth control circuit and built-in resistance compensator for achieving stable and fast charging," *IEEE Trans. Circuits Syst. I, Reg. Papers*, vol. 57, no. 2, pp. 506–517, Feb. 2010.

[4] J. C. Bendien, G. Fregien, and J. D. Wyk, "High-efficiency on-board battery charger with transformer isolation, sinusoidal input current and maximum power factor," *Proc. Inst. Elect. Eng. B—Elect. Power Appl.*, vol. 133, no. 4, pp. 197–204, Jul. 1986.

[5] B. Y. Chen and Y. S. Lai, "New digital-controlled technique for battery charger with constant current and voltage control without current feedback," *IEEE Trans. Ind. Electron.*, vol. 59, no. 3, pp. 1545–1553, Mar. 2012.

[6] Y. H. Liu and Y. F. Luo, "Search for an optimal rapid-charging pattern for Li-ion batteries using the Taguchi approach," *IEEE Trans. Ind. Electron.*, vol. 57, no. 12, pp. 3963–3971, Dec. 2010.

[7] Y. H. Liu, C. H. Hsieh, and Y. F. Luo, "Search for an optimal five-step charging pattern for Li-ion batteries using consecutive orthogonal arrays," *IEEE Trans. Energy Convers.*, vol. 26, no. 2, pp. 654–661, Jun. 2011.

[8] H. Surmann, "Genetic optimization of a fuzzy system for charge batteries," *IEEE Trans. Ind. Electron.*, vol. 43, no. 5, pp. 541–548, Oct. 1996.

[9] Z. Ullah, B. Burford, and S. Dillip, "Fast intelligent battery charging: Neural-fuzzy approach," *IEEE Aerosp. Electron. Syst. Mag.*, vol. 11, no. 6, pp. 26–34, Jun. 1996.

[10] G. C. Hsieh, L. R. Chen, and K. S. Huang, "Fuzzy-controlled Li-ion battery charge system with active state-of-charge controller," *IEEE Trans. Ind. Electron.*, vol. 48, no. 3, pp. 585–593, Jun. 2001.

[11] Y. H. Liu, J. H. Teng, and Y. C. Lin, "Search for an optimal rapid charging pattern for lithium-ion batteries using ant colony system algorithm," *IEEE Trans. Ind. Electron.*, vol. 52, no. 5, pp. 1328–1336, Oct. 2005.

[12] L. R. Chen, R. C. Hsu, and C. S. Liu, "A design of grey-predicted Li-ion battery charge system," *IEEE Trans. Ind. Electron.*, vol. 55, no. 10, pp. 3692–3701, Oct. 2008.

[13] L. R. Chen, "PLL-based battery charge circuit topology," *IEEE Trans. Ind. Electron.*, vol. 51, no. 6, pp. 1344–1346, Dec. 2004.

[14] L. R. Chen, C. S. Liu, and J. J. Chen, "Improving phase-locked battery charger speed by using resistance-compensated technique," *IEEE Trans. Ind. Electron.*, vol. 56, no. 4, pp. 1205–1211, Apr. 2009.

[15] L. R. Chen and C. S. Wang, "Modeling, analyzing and designing of a phase-locked charger," *J. Chin. Inst. Eng.*, vol. 30, no. 6, pp. 1037–1046, 2007.

[16] F. Savoye, P. Venet, M. Millet, and J. Groot, "Impact of periodic current pulses on lithium-ion batteryperformance," *IEEE Trans. Ind. Electron.*, to be published.

[17] L. R. Chen, J. J. Chen, N. Y. Chiu, and G. Y. Han, "Current-pumped battery charger," *IEEE Trans. Ind. Electron.*, vol. 55, no. 6, pp. 2482–2488, Jun. 2008.

[18] Y. C. Chuang, "High-efficiency ZCS buck converter for rechargeable batteries," *IEEE Trans. Ind. Electron.*, vol. 57, no. 7, pp. 2463–2472, Jul. 2010.

[19] L. R. Chen, C. M. Young, N. Y. Chu, and C. S. Liu, "Phase-locked bidirectional converter with pulse charge function for 42-V/14-V dual-voltage powernet," *IEEE Trans. Ind. Electron.*, vol. 58, no. 5, pp. 2045–2048, May 2011.

[20] Z. Jiang and R. A. Dougal, "Synergetic control of power converters for pulse current charging of advanced batteries from a fuel cell power source," *IEEE Trans. Power Electron.*, vol. 19, no. 4, pp. 1140–1150, Jul. 2004.

[21] H. J. Chiu, L. W. Lin, P. L. Pan, and M. H. Tseng, "A novel rapid charger for lead–acid batteries with energy recovery," *IEEE Trans. Power Electron.*, vol. 21, no. 3, pp. 640–647, May 2006.

[22] L. R. Chen, N. Y. Chu, and C. S. Wang, "Design of a reflex-based bidirectional converter with the energy recovery function," *IEEE Trans. Ind. Electron.*, vol. 55, no. 8, pp. 3022–3029, Jul. 2008.

[23] M. Bhatt, W. G. Hurley, and W. H. Wölfle, "A new approach to intermittent charge of valve-regulated lead–acid batteries in standby applications," *IEEE Trans. Ind. Electron.*, vol. 52, no. 5, pp. 1337–1342, Oct. 2005.

[24] M. Charkhgard and M. Farrokhi, "State-of-charge estimation for lithium-ion batteries using neural networks and EKF," *IEEE Trans. Ind. Electron.*, vol. 57, no. 12, pp. 4178–4187, Dec. 2010.

[25] L. R. Chen, "Design of duty-varied voltage pulse charger for improving Li-ion battery charging response," *IEEE Trans. Ind. Electron.*, vol. 56, no. 2, pp. 480–487, Feb. 2009.

[26] F. Lacressonni, B. Cassoret, and J. F. Brudny, "Influence of a charging current with a sinusoidal perturbation on the performance of a lead–acid battery," *Proc. Inst. Elect. Eng.—Elect. Power Appl.*, vol. 152, no. 5, pp. 1365–1370, Sep. 2005.

[27] L. R. Chen, S. L. Wu, and T. R. Chen, "Improving battery charging performance by using sinusoidal current charging with the minimum AC impedance frequency," in *Proc. IEEE ICSET*, Dec. 2010, pp. 1–4.

[28] W. G. Hurley, Y. S. Wong, and W. H. Wolfle, "Self-equalization of cell voltages to prolong the life of VRLA batteries in standby applications," *IEEE Trans. Ind. Electron.*, vol. 56, no. 6, pp. 2115–2120, Jun. 2009.

[29] K. A. Smith, C. D. Rahn, and C. Y. Wang, "Model-based electrochemical estimation and constraint management for pulse operation of lithium ion batteries," *IEEE Trans. Control Syst. Technol.*, vol. 18, no. 3, pp. 654–663, May 2010.

[30] A. A. H. Hussein and I. Batarseh, "A review of charging algorithms for nickel and lithium battery chargers," *IEEE Trans. Veh. Technol.*, vol. 60, no. 3, pp. 830–838, Mar. 2011.

[31] L. R. Chen, "A design of optimal pulse charge system by variable frequency technique," *IEEE Trans. Ind. Electron.*, vol. 54, no. 1, pp. 398–405, Feb. 2007.

[32] S. Buller, M. Thele, R. W. A. A. D. Doncker, and E. Karden, "Impedance-based simulation models of supercapacitors and Li-ion batteries for power electronic applications," *IEEE Trans. Ind. Appl.*, vol. 41, no. 3, pp. 742–747, Jun. 2005.

[33] M. Coleman, C. K. Lee, C. Zhu, and W. G. Hurley, "State-of-charge determination from EMF voltage estimation: Using impedance, terminal voltage, and current for lead–acid and lithium-ion batteries," *IEEE Trans. Ind. Electron.*, vol. 54, no. 5, pp. 2550–2557, Oct. 2007.

[34] D. V. Do, C. Forgez, K. E. K. Benkara, and G. Friedrich, "Impedance observer for a Li-ion battery using Kalman filter," *IEEE Trans. Veh. Technol.*, vol. 58, no. 8, pp. 3930–3937, Oct. 2009.

[35] F. Huet, "A review of impedance measurements for determination of the state-of-charge or state-of-health of secondary batteries," *J. Power Sources*, vol. 70, no. 1, pp. 59–69, Jan. 1998.

[36] S. M. R. Niya, M. Hejabi, and F. Goba, "Estimation of the kinetic parameters of processes at the negative plate of lead–acid batteries by impedance studies," *J. Power Sources*, vol. 195, no. 17, pp. 5789–5793, Sep. 2010.
[37] S. Rodrigues, N. Munichandriah, and A. K. Shukla, "AC impedance and state-of-charge analysis of a sealed lithium-ion rechargeable battery," *J. Solid State Electrochem.*, vol. 3, no. 7/8, pp. 397–405, Sep. 1999.
[38] F. Croce, F. Nobili, A. Deptula, W. Lada, R. Tossici, A. D'Epifanio, B. Scrosati, and R. Marassi, "An electrochemical impedance spectroscopic study of the transport properties of $LiNi_{0.75}Co_{0.25}O_2$," *Electrochem. Commun.*, vol. 1, no. 12, pp. 605–608, Dec. 1999.
[39] R. M. Spotniz, "AC impedance simulation for lithium-ion cells," in *Proc. 35th Int. Power Sources Symp.*, Jun. 1992, pp. 99–102.
[40] D. Qu, "The AC impedance studies for porous MnO_2 cathode by means of modified transmission line model," *J. Power Sources*, vol. 102, no. 1/2, pp. 270–276, Dec. 2001.
[41] J. Zhang, J. Yu, C. Cha, and H. Yang, "The effects of pulse charging on inner pressure and cycling characteristics of sealed Ni/MH batteries," *J. Power Sources*, vol. 136, no. 1, pp. 180–185, Sep. 2004.
[42] K. W. E. Cheng, B. P. Divakar, H. Wu, K. Ding, and H. F. Ho, "Battery-management system (BMS) and SOC development for electrical vehicles," *IEEE Trans. Veh. Technol.*, vol. 60, no. 1, pp. 76–88, Jan. 2011.
[43] M. B. Camara, H. Gualous, F. Gustin, A. Berthon, and B. Dakyo, "DC/DC converter design for supercapacitor and battery power management in hybrid vehicle applications-polynomial control strategy," *IEEE Trans. Ind. Electron.*, vol. 57, no. 2, pp. 587–597, Feb. 2010.
[44] N. Kularatna, "Rechargeable batteries and their management," *IEEE Instrum. Meas. Mag.*, vol. 14, no. 2, pp. 20–33, Apr. 2011.
[45] L. Wei, G. Joos, and J. Belanger, "Real-time simulation of a wind turbine generator coupled with a battery supercapacitor energy storage system," *IEEE Trans. Ind. Electron.*, vol. 57, no. 4, pp. 1137–1145, Apr. 2010.
[46] H. Fakham, L. Di, and B. Francois, "Power control design of a battery charger in a hybrid active PV generator for load-following applications," *IEEE Trans. Ind. Electron.*, vol. 58, no. 1, pp. 85–94, Jan. 2011.
[47] M. Pahlevaninezhad, J. Drobnik, P. K. Jain, and A. Bakhshai, "A load adaptive control approach for a zero-voltage-switching DC/DC converter used for electric vehicles," *IEEE Trans. Ind. Electron.*, vol. 59, no. 2, pp. 920–933, Feb. 2012.
[48] L. Ulrich, "State of charge," *IEEE Spectrum*, vol. 49, no. 1, pp. 5–59, Jan. 2012.

Liang-Rui Chen (M'04) was born in Changhua, Taiwan, in 1971. He received the B.S., M.S., and Ph.D. degrees in electronic engineering from the National Taiwan University of Science and Technology, Taipei, Taiwan, in 1994, 1996, and 2001, respectively.

In August 2006, he joined the faculty of the Department of Electrical Engineering, National Changhua University of Education, Changhua, where he is currently a Professor. His major research interests are power electronics, battery-powered circuit design, and renewable energy.

Shing-Lih Wu (S'09) was born in Taichung, Taiwan, in 1969. He received the B.S. degree from National Formosa University, Huwei, Taiwan, in 2003 and the M.S. degree from the Department of Electrical Engineering, Feng Chia University, Taichung, in 2005. He is currently working toward the Ph.D. degree in the Department of Electrical Engineering, National Changhua University of Education, Changhua, Taiwan.

His research interests include microcontroller control, battery charger, and control applications.

Deng-Tswen Shieh was born in Tainan, Taiwan, in 1968. He received the B.S., M.S., and Ph.D. degrees in chemical engineering from the National Taiwan University of Science and Technology, Taipei, Taiwan, in 1990, 1992, and 1995, respectively.

In 2002, he joined the Material and Chemical Research Laboratories, Industrial Technology Research Institute, Hsinchu, Taiwan, where he is currently a Researcher. His major research interests are safety and reliability of lithium-ion batteries/modules.

Tsair-Rong Chen received the B.S. and M.S. degrees in electrical engineering from National Cheng Kung University, Tainan, Taiwan, in 1986 and 1988, respectively, and the Ph.D. degree in electrical engineering from National Sun Yat-Sen University, Kaohsiung, Taiwan, in 1991.

In 1991, he was an Associate Professor with the Department of Electrical Engineering, National Changhua University of Education, Changhua, Taiwan, where he became a Professor in 1997. In 2001, he was the Chairman of Electrical Engineering with National Changhua University of Education, where he is currently the Dean of the College of Extension Education. His research interests include power electronics, battery charger, contactless power transfer, and microprocessor-based system design.